Journal of Power Sources 189 (2009) 127–132

Contents lists available at ScienceDirect

Journal of Power Sources

journal homepage: www.elsevier.com/locate/jpowsour

New insight into the discharge process of sulfur cathode by electrochemical impedance spectroscopy

Lixia Yuan, Xinping Qiu*, Liquan Chen, Wentao Zhu

Key Laboratory of Organic Optoelectronics and Molecular Engineering, Department of Chemistry, Tsinghua University, Beijing 100084, China

ARTICLE INFO

Article history:
Received 28 June 2008
Received in revised form
27 September 2008
Accepted 8 October 2008
Available online 18 October 2008

Keywords:
Lithium sulfur cells
Electrochemical impedance spectroscopy
Sulfur cathode
Equivalent circuits

ABSTRACT

In this paper, the electrochemical reactions of sulfur cathode during discharge–charge process were investigated by EIS technique combining with XRD, SEM and EDS methods. The discharge process of the sulfur cathode could be divided into two discharge regions. These are the first discharge region (2.5–2.05 V) where the reduction of elemental sulfur to form soluble polysulfides and further reduction of the soluble polysulfides occurs, and the second discharge region (2.05–1.5 V) where the soluble polysulfides are reduced to form a Li_2S solid film covered over the carbon matrix. It was found that the EIS can distinguish the individual contributions of charge transfer resistances, ion diffusion impedance and properties originating from Li_2S film in the frequency domain of 100 kHz to 100 mHz. During the upper voltage plateau, the impedance of interfacial charge transfer dominates the reduction reaction, while during the lower voltage plateau, the mass transport in the cathode is a control step. It was also proved that the solid Li_2S appeared at the beginning of the lower voltage plateau region and became denser during the following discharge process.

1. Introduction

Development of high energy density rechargeable batteries is becoming more and more important because of the increasing energy consumption of portable and transport applications [1]. For all the redox couples enabling for rechargeable batteries, Li/S couple has almost the highest specific-energy of 2600 Wh kg^{-1} [2,3], because the theoretical capacity of sulfur is the highest (1672 mAh g^{-1}) among all the possible solid compounds known for primary and rechargeable cathodes. In addition to the high capacity, elemental sulfur also has advantages of natural abundance, low cost and low toxicity, which are all the important factors for next generation of lithium batteries.

However, the realization of Li/S battery has a number of difficult problems to overcome. Typically, the biggest shortfall exhibited with these systems is a difficulty to sustain long cycle life. Previous cyclic voltammetry and ultraviolet analyses suggest that the discharge reaction of sulfur always consists of stepwise reduction processes and generates various forms of intermediate polysulfides which can dissolve in the electrolyte and cause not only the active material loss but also the morphology change of the sulfur cathode and finally lead to a rapid irreversible capacity fading at repeated cycles [4–9].

In order to improve the electrochemical rechargeability of the sulfur electrodes, many research works have been carried out to develop a denser and firmer cathode for stabilizing the morphology of the carbon matrix [10–13] and to use organosulfur compounds [14,15] or sulfur-composite compounds [16,17] for alleviating the dissoluble loss of sulfur in liquid electrolytes. So far, some success of achieving reasonably good cycle life of 50 cycles has been reported [10,17]. However, cycle capability still remains the bottleneck to overcome for the realization of the Li/S cells.

Although the details of the redox process of the sulfur cathode still remain unclear, it is generally accepted that the electrolyte-insoluble fully discharged product Li_2S species which is electronically nonconductive, is responsible for the capacity fading during the charge–discharge cycles [18–20]. Therefore it is very important to study the details relating to the solid Li_2S during the charge–discharge process.

Electrochemical impedance spectroscopy (EIS) is always recognized as one of the most powerful tools for studying the various stages of the complicated mechanism which can be elucidated from the EIS response of the electrochemical reaction. In this paper, we try to use EIS to investigate the electrochemical process of sulfur electrode, especially those concerning the formation, growth and dissolution of the Li_2S. This paper reports our preliminary

* Corresponding author. Tel.: +86 10 62794234; fax: +86 10 62794234.
E-mail address: qiuxp@mail.tsinghua.edu.cn (X. Qiu).

0378-7753/$ – see front matter © 2008 Elsevier B.V. All rights reserved.
doi:10.1016/j.jpowsour.2008.10.033

results on the EIS response of the sulfur electrode during the first discharge–charge cycle at ambient temperature.

2. Experimental

2.1. Preparation of the cathode

All test samples of the sulfur electrode was composed of 60 wt.% elemental sulfur (Analytical grade, Shanghai, China) and 30 wt.% carbon black (CB, Jiaozuo, China) and 10 wt.% copolymer of vinylidene fluoride and hexafluoropropylene (PVDF-co-HFP) (Mw = 534,000, Aldrich). Sulfur, PVDF-co-HFP and CB in 1-methyl-2-pyrrolidinone (NMP) were mixed in a planetary ball mill for 5 h. The mixed slurry was casted onto an Al foil and dried in a vacuum at 70 °C for 24 h.

2.2. Electrochemical measurements

The testing cells had a typical three-electrode construction using lithium foils as both the counter and reference electrodes, Cellgard 2400 microporous membrane as separator and 1.0 M $LiN(CF_3SO_2)_2$ dissolved in dimethoxyethane (DME) and dioxolane (DOL) (1:1, v/v) as the electrolyte. The cells were assembled in an argon-filled glove box. Charge–discharge tests were carried out on a constant current charger at a current density of 100 mA g^{-1} in the voltage range 1.5–2.5 V vs. Li/Li^+. Ex-EIS measurement were performed using Solartron FRA 1255B frequency response analyzer in combination with the potentiostat within the frequency range of 100 kHz to 100 mHz at potentiostatic signal amplitudes of 5 mV.

2.3. Structural characterization

The composition changes occurring in the sulfur electrodes during discharge and charge were characterized by ex situ powder X-ray diffraction (XRD). The sulfur cathodes for XRD analysis were taken out from the charged cells, washed with anhydrous DME and then sealed in a polyethylene pouch to protect the electrode surface from environmental contaminations. The test cells were disassembled in glove box. The XRD measurements were performed using the Rigaku X-ray diffractometer with Cu Kα radiation source. The changes in the surface morphology of the cathode electrodes during charge–discharge cycles were examined by scanning electron microscopy (SEM) on a JSM-6301F system (Japan) coupled with energy-dispersive X-ray spectroscopy (EDX, Oxford Instrument). In EDS investigation, at least three measurements were conducted for each sample to calculate the average composition.

3. Results and discussion

The typical voltage profile of Li/S cell employing 1.0 M $LiN(CF_3SO_2)_2$-(DME + DOL) (1:1, v/v) electrolyte during the first discharge and charge is displayed in Fig. 1. The discharge curve shows two plateau potential regions based on the voltage profile. These are the upper discharge region in the range of 2.5–2.05 V and the lower discharge region in the range of 2.05–1.5 V. Calculated from the content of sulfur, the initial discharge capacity of the sulfur cathode is about 875 mAh g^{-1}, corresponding to a 52% utilization of sulfur. The overall discharge profile was quite similar to that using the glyme solvents-based electrolyte previously reported [19,21,22]. It seems to indicate that the sulfur cathode system using the DME–DOL-based electrolyte has the same discharge mechanism. In conjunction with the previous study on the Li/S cell applied glyme-based electrolyte, the discharge process can be presumably described as follows: the upper discharge region corresponds to the formation of soluble long-chain polysulfide by the reduction of elemental sulfur, and the lower voltage region corresponds to the further reduction of the soluble polysulfide followed by formation of solid reduction product on carbon matrix. The suggested reduction process of sulfur cathode, which includes the phase separation of the sulfur species, seems to be very complex. In order to understand the redox process of the sulfur electrode, we investigated the EIS response of the sulfur cathode during the discharge–charge process accompanied with SEM, EDS, and XRD techniques. The samples for these measurements were made at the points indicated in the discharge profile (Fig. 1).

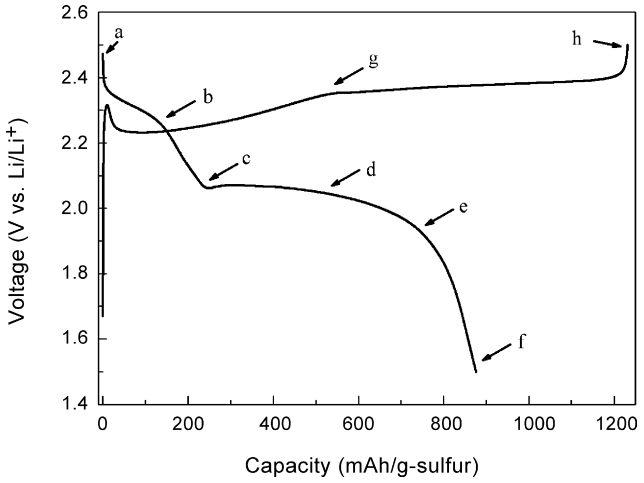

Fig. 1. The first discharge and charge curves of Li/S cell and the sulfur electrode samples during discharge–charge reaction process: (a) original, (b) 8% (130 mAh g^{-1}) discharge, (c) 14% (240 mAh g^{-1}) discharge, (d) 30% (500 mAh g^{-1}) discharge, (e) 46% (770 mAh g^{-1}) discharge, (f) 52% (870 mAh g^{-1}) discharge, (g) 30% (480 mAh g^{-1}) charge and (h) 75% charge (all calculated from the theoretical capacity of sulfur).

EIS measurements for the sulfur electrode at different discharge state were carried out. Fig. 2 shows the resulting impedance spectra. It can be seen from the figure that the impedance spectra can be divided into two types according to the shape of the curves. One type of impedance curves (see Fig. 2A) are composed of one depressed semicircle in high and a short inclined line in low frequency regions. While the other type of impedance spectra (see Fig. 2B) exhibit two depressed semicircles followed by a long sloping line. Furthermore, we notice that these two types of impedance spectra are corresponding to the two discharge plateau potential regions, respectively. In conjunction with the supposed reaction mechanism mentioned above, an assumption was given that the semicircle in the middle frequency range could be attributed to the formation of Li_2S (or Li_2S_2) on the carbon matrix in the cathode. If the assumption is correct, the semicircle in the middle frequency region can be used to monitor the formation, growth and dissolution of the solid products. The semicircle in the high frequency region should reflect the charge transfer process at the conductive agent interface. Based on these assumptions, those two types impedance spectra in Fig. 2 can be analyzed respectively with the equivalent circuits 1 and 2 shown in Fig. 3. In the equivalent circuits, Re represents the impedance contributed by the resistance of the electrolyte, Rct is the charge transfer resistance at the conductive agent interface, and CPE is a constant phase element which is used instead of capacitance, to take into account the roughness of the particle surface. The CPE1 is used instead of double-layer capacitance (Cdl), CPE2 describes the space charge capacitance of the Li_2S (or Li_2S_2) film and Rg is the resistance in the Li_2S (or Li_2S_2) film. Z_W is the Warburg impedance due to the diffusion of the polysulfides within the cathode. The fitting results are shown in Fig. 2, too.

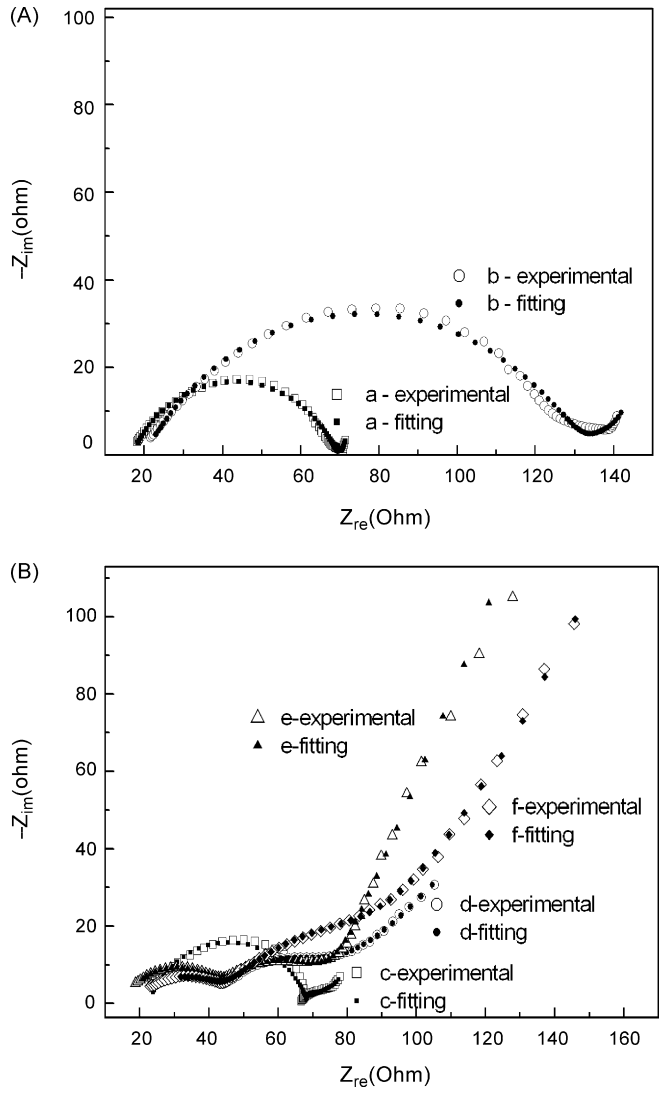

Fig. 2. Nyquist plots for sulfur electrode in the frequency range of (100 mHz–100 kHz) as a function of discharge: (A) upper plateau potential and (B) lower plateau potential.

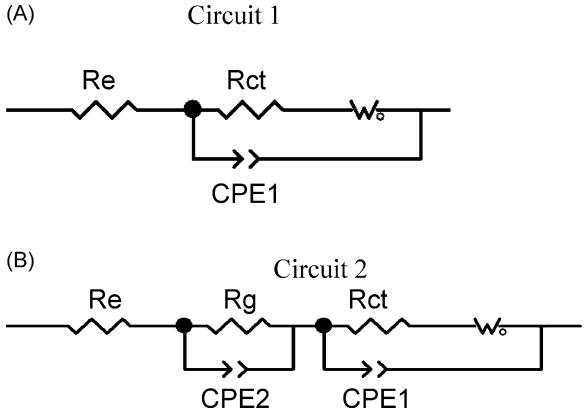

Fig. 3. The equivalent circuits used to fit the impedance spectra of Fig. 2.

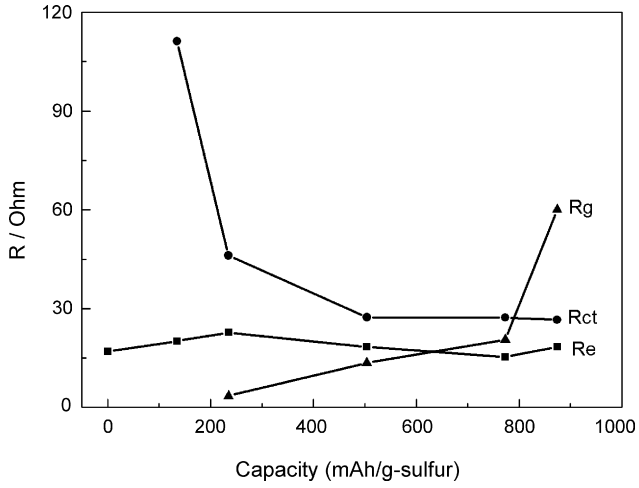

Fig. 4. Plots of Re, Rct and Rg vs. depth of discharge. (Parameters were obtained by modeling the impedance spectra in Fig. 2 with the equivalent circuits given in Fig. 3.)

Parameters of interest obtained from the simulation of the data according to the equivalent circuits are summarized in Fig. 4. The Rct of the original cell (curves as shown in Fig. 2A) which mainly implies the bulk impedance and interfacial impedance is not taken into account. Fig. 4 shows the dependences of Re, Rct, and Rg on the cathode's state of discharge. Although all of these three parameters change with the cathode's state of discharge, the trends are various. There is a little fluctuation with Re during the discharge process which should be caused by the dissolution of the polysulfides. The concentration of the polysulfides changes with the cathode's state of discharge, which means that the composition of the electrolyte is a function of the sulfur electrode's state at any given time. This makes difficulty for a lithium anode to form a stable SEI film which is responsible for the cycle efficiency of the lithium electrode. This is another reason for the poor cycle performance of the Li/S system. As to the Rct, there is a significant decrease from the 8% DOD to 14% DOD which is corresponding to the upper plateau and the beginning of the lower plateau, respectively. This means the charge transfer occurred in the reaction $S \rightarrow Li_2S_x$ ($8 \geq x \geq 4$) is more difficult than the charge transfer occurred in the reaction $Li_2S_{x1} \rightarrow Li_2S_{x2}$ ($8 \geq x1 > x2 \geq 4$). The reasons may be the insulating nature of elemental sulfur [23] and the poor electrical contact which lead to a poor electrochemical accessibility. While during the DOD range from 14% to 52%, the values of Rct are similar. This indicates that the charge transfer in the reaction $Li_2S_y \rightarrow Li_2S$ is not more difficult than the charge transfer in reaction $Li_2S_x \rightarrow Li_2S_y$ ($8 \geq x,y > 2$ and $x > y$). Unlike Re and Rct, Rg increased monotonously with the discharge process going on. Combining Fig. 3, Fig. 2 with Fig. 1, we can draw a conclusion that the solid Li_2S (or Li_2S_2) appeared at the very beginning of the second voltage plateau and became more and more severe during the following discharge process. The Li_2S (or Li_2S_2) film which deposits on the carbon matrix can cause a serious Warburg impedance due to the polysulfides diffusion within the cathode (see Fig. 2B). Both the interfacial charge transfer and the mass transport contribute to the electrochemical reactions. From a kinetic point of view, we can describe the discharge process of the sulfur cathode like this: during the upper voltage plateau, the impedance of interfacial charge transfer dominate the reduction reaction, while during the lower voltage plateau, the mass transport in the cathode is a control step.

All of the above analyses are based on the assumption that the semicircle in the middle frequency range is caused by the film of Li_2S (or Li_2S_2) on the carbon matrix in the cathode. To validate this assumption, we investigated the morphology and composition

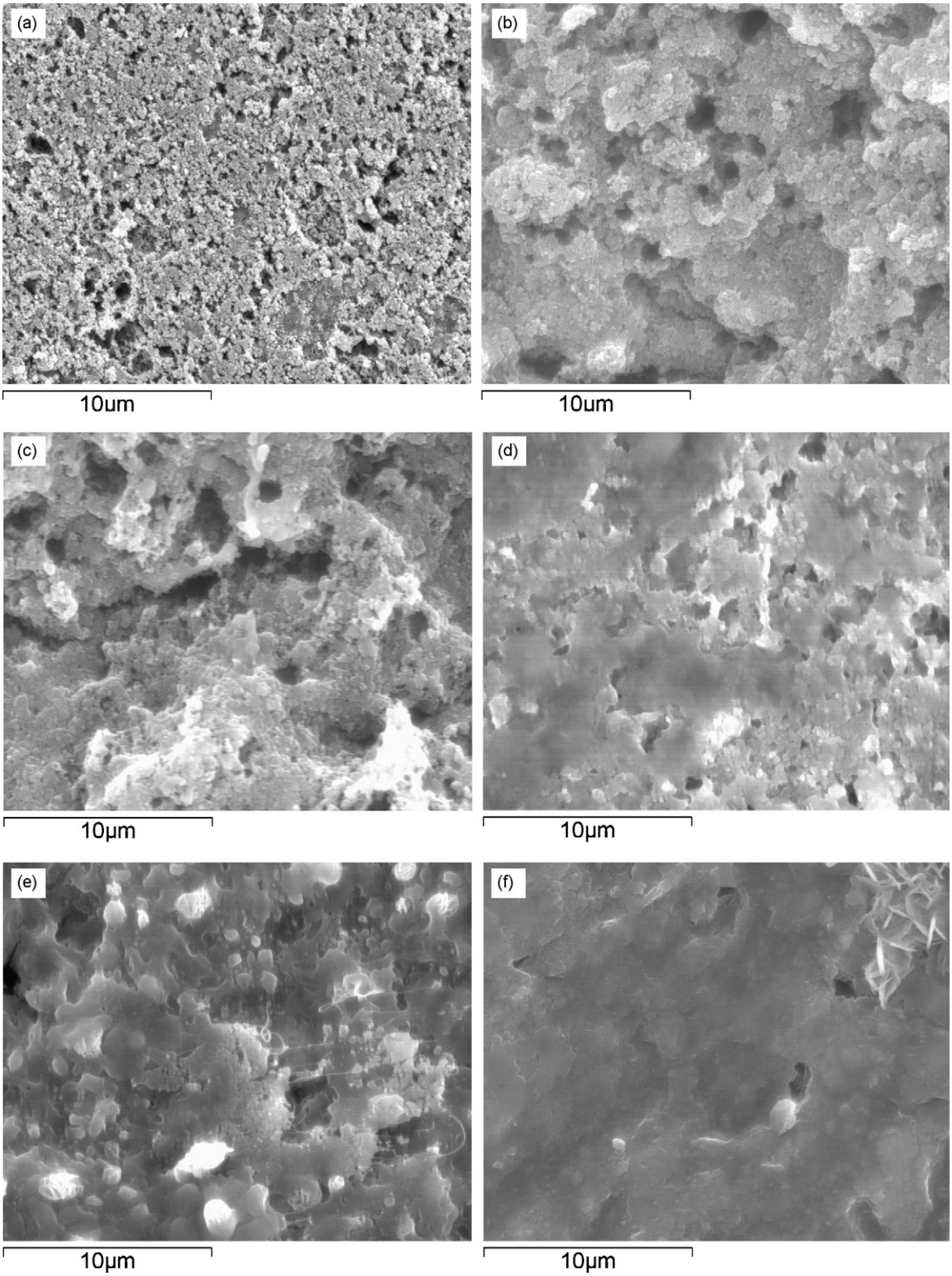

Fig. 5. SEM images of the sulfur cathode during the first discharge process (a–f are all corresponding to the points indicated in Fig. 1).

changes in the sulfur cathode during discharge by means of SEM, EDS and XRD techniques.

Fig. 5 shows the SEM images of the cathode at different depth of discharge. Before SEM measurements, the remaining soluble polysulfides in the cathode was completely washed with DME. Therefore, only solid compounds were observed in the SEM images. Prior to discharge, the original sulfur electrode represented homogenous mixing of sulfur, carbon and PVDF (see Fig. 5a). At the middle point of the 2.4 V plateau, most of the sulfur particles disappeared in the cathode as can be seen in Fig. 5b. Until the end of the first discharge region, there is little solid reduction product can be observed in the cathode, as shown in Fig. 5c, only carbon matrix

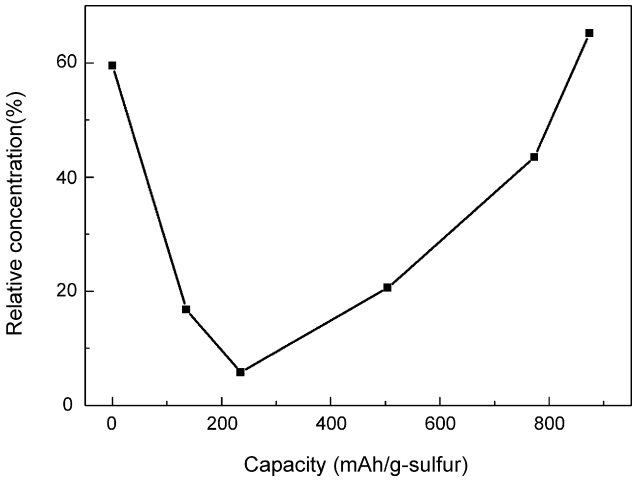

Fig. 6. Relative content (by EDS) of sulfur during the first discharge process.

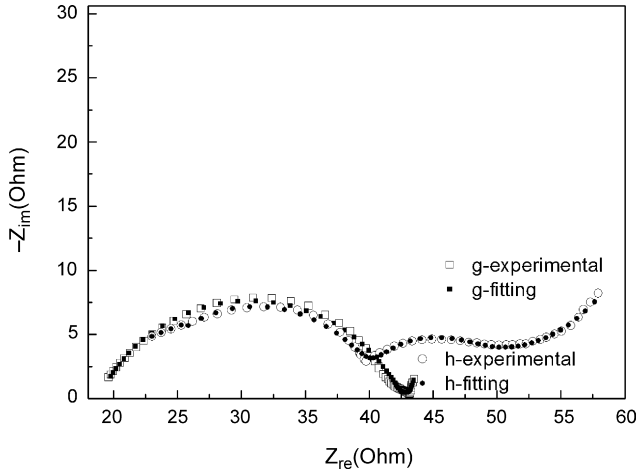

Fig. 8. Nyquist plots for sulfur electrode in the frequency range of (100 kHz–100 mHz) as a function of charge.

was observed at the end of the first discharge region. However, there was a significant change in the cathode at the middle part of the 2.05 V plateau. The surface of the carbon matrix was significantly covered with a solid film (see Fig. 5d). And the passivation caused by the solid film became denser during the following discharge (see Fig. 5e and f).

The content of the sulfur and the solid-state reduction product in the cathode was semiquantitatively determined by means of EDS measurement which was implemented with SEM. As shown in Fig. 6, the relative sulfur content in the cathode decreases abruptly during the first discharge region, and then increases in the second discharge region. These results are in good agreement with the results of the SEM measurement. The decrease of the sulfur content in the first discharge region can be attributed to the decrease of the solid elemental sulfur by the formation of the soluble polysulfides, and the increase of the sulfur content in the second discharge region would be associated with the generation of the Li_2S (or Li_2S_2) on the carbon matrix.

The changes of XRD patterns are displayed in Fig. 7. The original sulfur electrode (see Fig. 7a) represents an orthorhombic structure. The peak area of sulfur drastically decreased with the discharge going on (see Fig. 7b) and disappeared at the end of the upper plateau (Fig. 7c). At the lower plateau region (Fig. 7d–f), we could find out new peaks which were coincided with Li_2S. These peaks of Li_2S became stronger with the discharge going on, which should be contributed to the increasing amount of Li_2S.

There is no evidence given by the measurements of SEM, EDS and XRD that the formation of Li_2S begins at the beginning of the lower plateau region (or the end of the upper plateau region). This seems to be little inconsistent with the assumption of the EIS model mentioned above. There are two possible reasons. One is that the EIS equivalent circuit is unreasonable for the discharge reaction of sulfur. The other is that those methods, such as SEM and XRD, are not sensitive enough to study the details of the electrochemical reaction.

To answer this question, EIS measurements for the sulfur electrode at different charge state corresponding to the points indicated in the charge profile (see Fig. 1) were carried out. The resulting impedance features are shown in Fig. 8. According to the previous study on Li/S batteries, we know that when recharging after the very first discharge, polysulfides do not transform back into elemental sulfur even at 100% depth of charge [19,24].

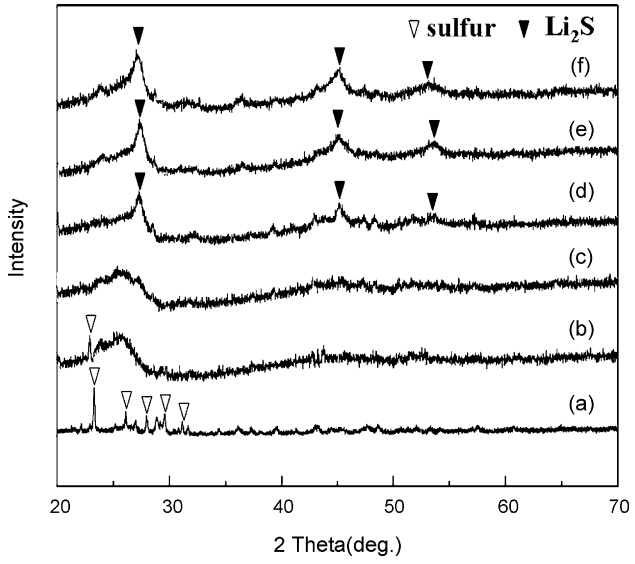

Fig. 7. The XRD pattern of sulfur electrode during the first discharge process.

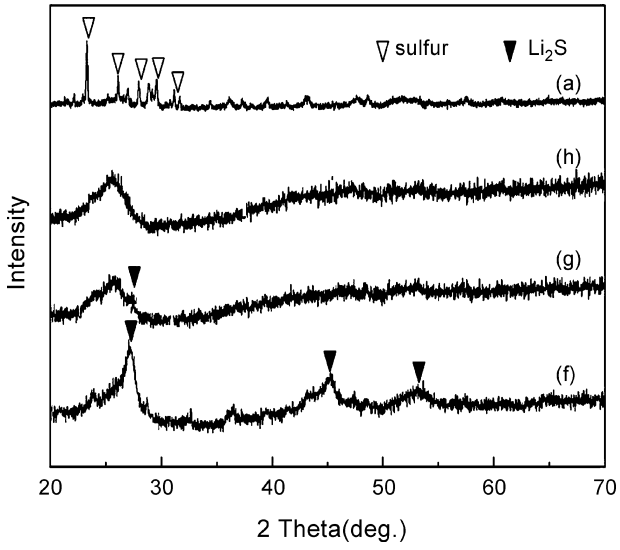

Fig. 9. The XRD pattern of sulfur electrode during the first charge process.

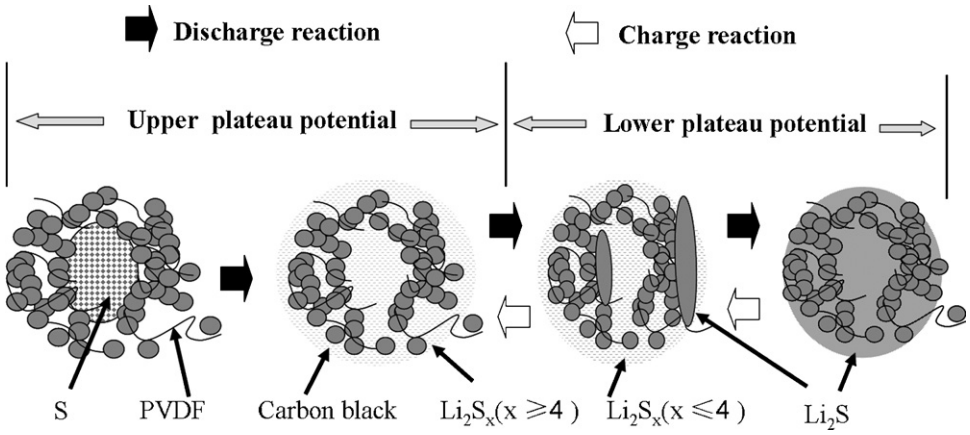

Fig. 10. The discharge and charge reaction model of sulfur cathode.

Based on the model that the semicircle in the middle frequency range is caused by the solid Li_2S (or Li_2S_2) film on the carbon matrix in the cathode, the impedance spectra of the fully charged cathode should display only one semicircle. The EIS experiment result displayed in Fig. 8 is in good agreement with the hypothesis which confirms that the EIS model given above can depict the electrochemical reaction process of sulfur cathode properly. Fig. 9 also gives XRD patterns of the 'sulfur' electrode at different charge state. As expected, for the fully charged 'sulfur' electrode, the Li_2S disappeared and elemental sulfur was not detected. The obtained results may further confirm that EIS is a powerful technique to study the fundamental processes in sulfur cathode due to the electrochemical nature of the charge–discharge reaction.

According to the results discussed above, the model of the sulfur cathode during discharge–charge cycles can be shown as Fig. 10. During the very first discharge, the elemental sulfur changed to polysulfides at upper plateau region, and polysulfides transformed to Li_2S at the lower plateau region. When recharging, Li_2S only recovered long chain polysulfides not elemental sulfur even at 100% depth of charge.

4. Conclusions

EIS was proved to be a powerful technique to study the details of the electrochemical reaction of sulfur cathode during charge–discharge process. The individual contributions of charge transfer resistances, ion diffusion impedance and properties originated from the Li_2S film were distinguished in the frequency domain. The obtained results are summarized as follows:

1. The semicircle in the middle frequency range was found to be caused by the Li_2S film on the carbon matrix in the cathode.
2. Solid Li_2S appeared at the beginning of the lower voltage plateau region and became denser during the following discharge process.
3. During the upper voltage plateau, the impedance of interfacial charge transfer dominate the reduction reaction, while during the lower voltage plateau, the mass transport in the cathode is a control step.

Acknowledgements

The authors gratefully acknowledge the financial support by the National Natural Science Foundation of China (20803042) and the National 973 Program, China (Grant No. 2009CB220105).

References

[1] A.G. Ritchie, J. Power Sources 136 (2004) 285.
[2] N. Petr, M. Klaus, K.S.V. Santhanam, H. Otto, Chem. Rev. 97 (1997) 207.
[3] M.Y. Chu, U.S. Pat. 5,814,420 (1998).
[4] H. Yamin, A. Gorenshtein, J. Penciner, Y. Sternberg, E. Peled, J. Electrochem. Soc. 135 (1988) 1045.
[5] D. Marmorstein, T.H. Yu, K.A. Striebel, F.R. McLarnon, J. Hou, E.J. Cairns, J. Power Sources 89 (2000) 219.
[6] D.H. Han, B.S. Kim, S.J. Choi, Y. Jung, J. Kwak, S.M. Park, J. Electrochem. Soc. 151 (9) (2004) E283.
[7] E. Peled, A. Gorenshtein, M. Segal, Y. Sternberg, J. Power Sources 26 (1989) 269.
[8] J.R. Akridge, Y.V. Mikhaylik, N. White, Solid State Ionics 175 (2004) 243.
[9] S.E. Cheon, K.S. Ko, J.H. Cho, S.W. Kim, E.Y. Chin, H.T. Kim, J. Electrochem. Soc. 150 (2003) A800.
[10] Y. Jung, S. Kim, Electrochem. Commun. 9 (2007) 249.
[11] J. Sun, Y. Huang, W. Wang, Z. Yu, A. Wang, K. Yuan, Electrochem. Commun. 10 (2008) 930.
[12] Y.J. Choi, Y.D. Chung, C.Y. Baek, K.W. Kim, H.J. Ahn, J.H. Ahn, J. Power Sources 184 (2008) 548.
[13] J. Sun, Y. Huang, W. Wang, Z. Yu, A. Wang, K. Yuan, Electrochim. Acta 53 (2008) 7084.
[14] J.M. Pope, T. Sato, E. Shoji, N. Oyama, K.C. White, D.A. Buttry, J. Electrochem. Soc. 149 (7) (2002) A939.
[15] Y.J. Li, H. Zhan, L.B. Kong, Y.H. Zhou, Electrochem. Commun. 9 (2007) 1217.
[16] J. Wang, S.Y. Chew, Z.W. Zhao, S. Ashraf, D. Wexler, J. Chen, S.H. Ng, S.L. Chou, H.K. Liu, Carbon 46 (2008) 229.
[17] J.L. Wang, J. Yang, C.R. Wan, K. Du, J.Y. Xie, N.X. Xu, Adv. Funct. Mater. 13 (2003) 487.
[18] S.E. Cheon, J.H. Cho, K. Ko, C.W. Kwon, D.R. Chang, H.T. Kim, S.W. Kim, J. Electrochem. Soc. 149 (2002) A1437.
[19] S.E. Cheon, K.S. Ko, J.H. Cho, S.W. Kim, E.Y. Chin, H.T. Kim, J. Electrochem. Soc. 150 (2003) A796.
[20] S.E. Cheon, S.S. Choi, J.S. Han, Y.S. Choi, B.H. Jung, H.S. Lim, J. Electrochem. Soc. 151 (12) (2004) A2067.
[21] M.Y. Chu, L.C. De Jonghe, S.J. Visco, B.D. Katy, U.S. Pat. 6,030,720 (2000).
[22] J. Shim, K. Striebel, E. Cairns, J. Electrochem. Soc. 149 (2002) A1321.
[23] J.A. Dean (Ed.), Lange's Handbook of Chemistry, 3rd ed., McGraw-Hill, New York, 1985, pp. 3–5.
[24] Y.V. Mikhaylik, J.R. Akridge, J. Electrochem. Soc. 151 (11) (2004) A1969.